

1 **Flood frequency analysis at ungauged catchments with the GAM and**
2 **MARS approaches in the Montreal region, Canada**

3
4
5 Amina Msilini^{*,1}, Christian Charron¹, Taha B.M.J. Ouarda¹ and Pierre Masselot²

6
7
8 ¹Canada Research Chair in Statistical Hydro-Climatology, Institut national de la
9 recherche scientifique, Centre Eau Terre Environnement, 490 de la Couronne, Québec,
10 QC, G1K 9A9, Canada.

11 ²London School of Hygiene & Tropical Medicine (LSHTM), Keppel Street London,
12 WC1E 7HT, United Kingdom.

13
14
15
16
17 *Corresponding author: Amina Msilini (Amina.Msilini@ete.inrs.ca;
18 amina.msilini.m@gmail.com).

19
20
21
22
23
24
25

26 **January, 2022**

27 **Flood frequency analysis at ungauged catchments with the GAM and**
28 **MARS approaches in the Montreal region, Canada**

29 **Abstract**

30 Regional frequency analysis (RFA) aims to estimate quantiles of extreme hydrological
31 variables (e.g. floods or low-flows) at sites where little or no hydrological data is
32 available. This information is of interest for the optimal planning and management of
33 water resources. A number of regional estimation models are evaluated and compared in
34 this study and then used for regional estimation of flood quantiles at ungauged
35 catchments located in the Montreal region in southern Quebec, Canada. In this study, two
36 neighborhood approaches using canonical correlation analysis (CCA) and the region of
37 influence (ROI) method are applied to delineate homogenous regions. Three regression
38 methods namely log-linear regression model (LLRM), generalized additive models
39 (GAM), and multivariate adaptive regression splines (MARS), recently introduced in the
40 RFA context, are considered for regional estimation. These models are also applied
41 considering all stations (ALL). The considered models, especially MARS, have never
42 been used previously in a concrete application. Results indicate that MARS and GAM
43 have comparable predictive performances, especially when applied with the whole
44 dataset. Results also show that MARS used in combination with the CCA approach
45 provide improved performances compared to all considered regional approaches. This
46 may reflect the flexibility of the combination of these two approaches, their robustness,

47 and their ability to better reproduce the hydrological phenomena, especially in real-world
48 conditions when limited data are available.

49 **Résumé**

50 L'analyse fréquentielle régionale (AFR) vise à estimer les quantiles de variables
51 hydrologiques extrêmes (par exemple, les crues ou les étiages) sur des sites avec peu ou
52 aucune information hydrologique de disponible. Ces informations sont intéressantes pour
53 la planification et la gestion optimales des ressources en eau. Un certain nombre de
54 modèles d'estimation régionale ont été évalués et comparés dans cette étude, puis utilisés
55 pour l'estimation régionale des quantiles de crue dans des bassins versants non jaugés
56 situés dans la région de Montréal dans le sud du Québec, Canada. Dans cette étude, deux
57 approches d'identification de voisinage utilisant l'analyse canonique de corrélation
58 (CCA) et la méthode de la région d'influence (ROI) sont appliquées pour délimiter des
59 régions homogènes. Trois méthodes de régression, à savoir le modèle de régression log-
60 linéaire (LLRM), les modèles additifs généralisés (GAM) et la régression multivariée par
61 spline adaptative (MARS), récemment introduite dans le contexte de l'AFR, sont prises
62 en compte pour l'estimation régionale. Ces modèles sont également appliqués en
63 considérant toutes les stations (ALL). Les modèles considérés, en particulier MARS,
64 n'ont jamais été utilisés auparavant dans une application concrète. Les résultats indiquent
65 que MARS et GAM ont des performances prédictives comparables, en particulier
66 lorsqu'ils sont appliqués à l'ensemble de la base de données. Les résultats montrent
67 également que MARS utilisé en combinaison avec l'approche de CCA offre de meilleures
68 performances par rapport à toutes les approches régionales considérées. Cela peut refléter
69 la flexibilité de la combinaison de ces deux approches, leur robustesse et leur capacité à

70 mieux reproduire les phénomènes hydrologiques, en particulier dans des conditions
71 réelles lorsque des données limitées sont disponibles.

72 **Keywords:** Multivariate adaptive regression splines; Generalized additive models;
73 Montreal region (Canada); Ungauged basin; Regional frequency analysis; Drainage
74 network characteristics.

75 **1. Introduction**

76 Knowledge of the frequency and the magnitude of extreme hydrological events (e.g.
77 floods and low-flows) are of interest for water resources management and hydrological
78 design. Estimation of extreme flows is often required at sites where little or no
79 hydrological data is available. To this end, regional frequency analysis (RFA) approaches
80 are commonly used to estimate and assess extreme hydrological event characteristics.
81 Generally, RFA includes two main steps: i) delineation of homogenous regions (DHR) to
82 group gauged sites with hydrological behavior similar to the target one and ii) regional
83 estimation (RE) to transfer the information from gauged sites to the target one within the
84 same homogeneous region (e.g. Chebana and Ouarda 2008). Various methods have been
85 suggested and documented for each of these two steps (e.g. Ouarda 2016). In practice,
86 two DHR methods are often considered, namely : the region of influence (ROI) (Burn
87 1990) and the canonical correlation analysis (CCA) (Ouarda et al. 2001). The
88 geographical proximity of the catchments has also long been recognized and considered
89 in RFA to group sites with similar characteristics (Han et al. 2020). It is especially
90 convenient for practical purposes.

91 For the RE step, two main approaches have commonly been used to regionalize flood
92 characteristics. The first one includes regression-based approaches, where log-linear
93 regression models (LLRM) are the most used because of their simplicity and good
94 predictive performances. The second approach includes the index-flood models
95 (Dalrymple 1960), where it is assumed that in a given homogeneous region, all local data
96 normalized by a central position indicator (e.g. mean or median) have the same
97 distribution.

98 Hydrological processes represent complex and nonlinear natural phenomena (Xu et al.
99 2010). They depend on a large number of interactive physio-meteorological catchment
100 attributes such as the climate of the region, the topographic variability of the catchments,
101 their soil characteristics, and their geological formations. The log-linear method
102 commonly used in the RE step assumes that the relation between the response variable
103 and the explanatory variables is linear. This assumption is generally not satisfied in such
104 complex non-linear processes. To deal with the natural complexity of the hydrological
105 events and account for the presence of non-linearity between the explanatory and the
106 response variables, a number of non-linear approaches have been suggested in the
107 literature such as the artificial neural networks (ANNs) and the Generalized Additive
108 Models (GAMs) (e.g. Khalil, Ouarda, and St-Hilaire 2011; Ouarda et al. 2018). The use
109 of ANNs to regionalize extreme hydrological characteristics has become increasingly
110 popular (Ouarda and Shu 2009). However, it presents a major drawback which is the
111 tendency to overfit the data (e.g. Gal and Ghahramani 2016; Lawrence and Giles 2000).
112 Furthermore, their calibration is somewhat a complex task that requires some subjective
113 choices.

114 The use of GAM has also become increasingly popular in a number of fields such as
115 hydro-climatology and environmental modelling (e.g. Wen et al. 2011; Rahman et al.
116 2018), public health (e.g. Leitte et al. 2009; Bayentin et al. 2010), renewable energy
117 assessment (e.g. Ouarda et al. 2016) and hydrology (e.g. Rahman et al. 2018; López-
118 Moreno and Nogués-Bravo 2005). It has been recently introduced in the RFA context by
119 Chebana et al. (2014), where the authors found that GAM performs better than the
120 classical linear regression model. However, the method can be computationally intensive
121 and difficult to fit to high-dimensional databases (large number of explanatory variables).

122 The reliability of the regional flood characteristic estimates depends strongly on the
123 amount of available gauged sites data used in the regional estimation. In practice, it is
124 often the case that rivers are poorly monitored and/or they have a short time series.
125 Msilini et al. (2020) suggested that it may be possible to perform a reliable regional
126 estimation with MARS even using a few data in the RFA context. The application of
127 MARS in a real case study has never been performed.

128 The aim of the present paper is to develop and test a number of approaches listed above
129 in a practical real-world case study, with limited number of stations, consisting in the
130 estimation of flood quantiles at 11 ungauged sites of interest in the Montreal region
131 (Canada). Such quantiles are essential for the municipality to established flood maps
132 within the region. The catchments of the considered study region are often of small areas
133 and they are characterized by their high urbanized and agricultural areas which allow for
134 a very high runoff. Moreover, the hydrological response in the Montreal catchments is
135 known to have a higher degree of variability and non-linearity. Hence, the adoption of

136 non-linear RE models, especially, MARS in predicting flood discharge at ungauged
137 catchments in such conditions may be relevant.

138 In this study, the LLRM, GAM and MARS models are used in conjunction with/and
139 without the delineation of homogeneous region methods (ROI and CCA). Calibrations of
140 the regional models are performed with catchments located within a radius of 250
141 kilometres around the target area to ensure certain similarity between their catchment
142 characteristics. The performances of the different approaches are compared and the best
143 identified models are used to predict flood quantiles at the 11 target ungauged sites.

144 This paper is organized as follows. Section 2 presents a brief theoretical background of
145 the different RFA approaches adopted in this work. The considered methodology is
146 discussed in section 3. The case study and the dataset are described in section 4. The
147 obtained results are illustrated and discussed in section 5. Finally, the conclusions of the
148 study are summarized in section 6.

149 **2. Theoretical background**

150 ***2.1 Delineation of homogeneous region approaches***

151 *2.1.1 Canonical correlation analysis (CCA)*

152 CCA is a technique commonly used to identify the possible correlations between two
153 groups of random variables. Let $X=(X_1,X_2,\dots,X_r)$ and $Y=(Y_1,Y_2,\dots,Y_s)$ be sets of random
154 variables of respectively r physio-meteorological variables and s hydrological variables
155 of n gauged sites. CCA allows identifying the dominant linear modes of covariability

156 between the vectors X and Y so that it is possible to do inference about Y knowing X. Let
 157 V_i and W_i be linear combinations (called canonical variables) of the sets X and Y, i.e.:

$$V_i = A_{i1}X_1 + A_{i2}X_2 + \dots + A_{ir}X_r \quad (1)$$

$$W_i = B_{i1}Y_1 + B_{i2}Y_2 + \dots + B_{is}Y_s \quad (2)$$

158 where $i = 1, \dots, d$ and $d = \min(r, s)$. CCA allows for the identification of vectors A and B
 159 in such a way that the correlation coefficients between the canonical variables, i.e. $\lambda_i =$
 160 $\text{corr}(V_i, W_i)$ where $i = j$, is maximized and $\text{corr}(V_i, W_j) = 0$ where $i \neq j$ under constraints
 161 of unit variance.

162 In the RFA, the hydrological neighborhood for a given target ungauged site at $100(1 -$
 163 $\alpha)\%$ confidence level is defined by the set of K sites such that the canonical hydrological
 164 score w_k , $k = 1, \dots, K$, is close to the canonical physio-meteorological score of the
 165 target site v_0 . The closeness is measured using a Mahalanobis distance calculated
 166 between the hydrological mean position of the site of interest Λv_0 and the positions of
 167 other sites w_k such that :

$$(W - \Lambda V_0)^T (I_d - \Lambda^2)^{-1} (W - \Lambda V_0) \leq \chi^2_{\alpha, d} \quad (3)$$

168 where $\chi^2_{\alpha, d}$ is defined such that $\text{Prob}(\chi^2 \leq \chi^2_{\alpha, d}) = 1 - \alpha$, I_d is the $d \times d$ identity matrix and $\Lambda =$
 169 $\text{diag}(\lambda_1, \dots, \lambda_d)$. For more details the reader is referred to Ouarda et al. (2001).

170 2.1.2 Region of influence (ROI)

171 The ROI approach was introduced by Burn (1990). As the CCA technique, the ROI can
 172 be used in the RFA to identify the neighborhood of a given target site. In this method, the

173 identification of the neighborhood is carried out based on the similitude between
 174 catchment characteristics. The similitude is measured based on the Euclidean distance
 175 calculated in the physio-meteorological space (e.g. Burn 1990; Tasker, Hodge, and Barks
 176 1996) i.e.:

$$ROI_i = \left\{ \text{sites } j \in (1, \dots, n); D_{ij} = \left[\sum_{k=1}^r W_k (X_{k,i} - X_{k,j})^2 \right]^{\frac{1}{2}} \leq \Theta \right\} \quad (4)$$

177 where D_{ij} is the weighted Euclidean distance between the target site i and the gauged one,
 178 $j = 1, \dots, n$, $X_{k,j}$ ($k = 1, \dots, r$) is the standardized value of the k^{th} physio-meteorological
 179 variable at site j , W_k is the weight associated with the k^{th} physio-meteorological variable,
 180 and Θ represents the threshold value. For more details, the reader is referred to (e.g. Burn
 181 1990; GREHYS 1996).

182 **2.2 Regional estimation approaches**

183 **2.2.1 Log Linear Regression Model (LLRM)**

184 The log-linear regression model (LLRM) is one of the most common regional estimation
 185 models. It consists in establishing a linear relationship between the hydrological variable
 186 Y and the physio-meteorological characteristics of a given catchment (X_1, X_2, \dots, X_m)
 187 (e.g. Pandey and Nguyen, 1999) :

$$\log (E(Y/X)) = \beta_0 + \sum_{j=1}^m \beta_j \log (X_j) + \varepsilon \quad (5)$$

188 Where X is a matrix whose columns correspond to a set of m explanatory variables, β_0
 189 and β_j are unknown parameters to be estimated using the least-squares method, and ε is
 190 the model error.

191 2.2.2 *Generalized Additive Model (GAM)*

192 GAM (Hastie and Tibshirani 1987) is a non-linear model that is able to model a large
193 variety of nonlinear relationships and it allows to consider non-Gaussian response
194 variables (Wood 2006). This model uses flexible non-linear smooth functions to model
195 the response variable (i.e. the hydrological variable). A GAM can then be defined as
196 (Wood 2006):

$$g(E(Y/X)) = \alpha + \sum_{j=1}^m f_j(X_j) + \varepsilon \quad (6)$$

197 where g is a monotonic link function, X is a matrix whose columns correspond to a set of
198 m explanatory variables, and f_j are smooth functions giving the relationship between the
199 explanatory variables X_j and the response variable Y , α is the intercept and ε is the error
200 term. Because of the additive property of GAM, one can separately analyze the impact of
201 each explanatory variable on the response variable.

202 The smooth non-linear functions f_j are expressed as:

$$f_j(X) = \sum_{i=1}^q \beta_{ji} b_{ji}(X) \quad (7)$$

203 where β_{ji} are parameters to be estimated and b_{ji} are the spline basis functions. Further
204 information on GAM can be found in Wood (2006) and Wood (2017).

205 2.2.3 *Multivariate adaptive regression splines (MARS)*

206 Friedman (1991) introduced MARS as a flexible non-parametric regression approach able
207 to model complex and non-linear relationship often hidden in high-dimensional data. The
208 MARS model $f(X)$ can be defined as a linear combination of basis functions and their
209 interactions as:

$$f(X) = \beta_0 + \sum_{n=1}^r \beta_n B_n(X) \quad (8)$$

210 where β_0 is the intercept, and β_n are regression coefficients of the basis functions
211 ($B_n(X)$).

212 Three forms can be taken by the $B_n(X)$ terms in the MARS model: i) a constant term
213 which represents the intercept, ii) a linear spline functions on a given variable X_j namely
214 hinge function ($h_m(X_j) = (t_m - X_j)_+$ or $h_m(X_j) = (X_j - t_m)_+$ where t is a knot) or iii) a product
215 of two or more $h_m(X_j)$ which represents the interaction between the variables. The $B_n(X)$
216 are defined in pairs of $h_m(X_j)$ and are separated by a knot between the range of a given
217 variable.

218 MARS algorithm builds a model in two main steps: the first step is the forward pass
219 where the model starts with the intercept and iteratively adds the B_n s. At each time, the
220 most significant variable and knot yielding the largest decrease in the error of the model
221 are chosen. This step results in a large model that usually overfits the data. The second
222 step is the backward pass which allows improving the predictive performance of the built
223 model by deleting the less significant B_n s. This later step continues until obtaining the

224 best sub-models having the lowest Generalized Cross Validation (GCV) score. For more
225 details, the reader is referred to Msilini, Masselot, and Ouarda (2020).

226 **3. Methodology**

227 *3.1 Regional models*

228 In this work, two methods for neighborhood identification (CCA and ROI) are applied in
229 combination with the LLRM, GAM and MARS for regional estimation. Three other
230 approaches are also assessed by applying the LLRM, GAM and MARS using all stations
231 (ALL). Table 1 summarizes the used combinations.

232 The CCA and the ROI techniques are applied in the DHR step to improve the degree of
233 homogeneity, and hence the accuracy of the predictions of the RE models. For these
234 methods, the relevant variables in terms of explaining the flooding process need to be
235 identified. In this work, the appropriate variables selected for the LLRM with a stepwise
236 procedure approach are adopted in each of the neighborhood methods such as in Ouarda
237 et al. (2018). Then, the optimal number of sites in the neighborhood (optimum threshold
238 distance) is identified based on a jackknife procedure. This distance is the one that
239 minimizes a given performance criterion of the log-linear model applied in each
240 neighborhood.

241 GAM is fitted using the R package mgcv (Wood 2006). The thin plate regression spline is
242 considered in this study as a basis in the smoothing function. The adopted link function is
243 the identity function because of the approximately Gaussian log-transformed quantiles (
244 see Chebana et al. (2014), for instance).

245 MARS is built using the R package earth (Milborrow 2018). To this end, three main
246 parameters need to be tuned: the maximum number of terms to be reached in the model in
247 the forward phase (N_k), the degree of interaction between the variables (degree) which
248 allows including interaction terms between multiple hinge functions when its value is
249 greater than 1, and the maximum number of terms to be retained after the backward phase
250 (N_{prune}). These parameters are optimized based on the GCV, the residual sum of squares
251 (RSS) and the coefficient of determination (R^2) criteria of the fitted models. Imposing
252 termination conditions for the forward pass is necessary to save calculation time and to
253 avoid the generation of terms with arbitrary knots. This allows optimizing the model
254 more efficiently. In this study, the parameter N_k is optimized to avoid that the final model
255 includes a large number of variables. This may allow obtaining more reliable estimates
256 within the neighborhood.

257 For each regional model, different sets of physio-meteorological variables are considered.
258 A backward stepwise technique is used in this work to select the most significant
259 explanatory variables for each RE models (LLRM, GAM and MARS). The presentation
260 of this approach is given in the next section.

261 ***3.2 Variable selection***

262 The backward stepwise selection procedure is used in this study to identify the optimal
263 combination of explanatory variables as in Ouarda et al. (2018). This technique consists
264 in removing iteratively the least significant variable from an initial full model containing
265 all available variables. At each step, the deleted variable is the one associated with the
266 highest p -value for the null hypothesis that the coefficients β_j in Eq. (5) (for the LLRM)

267 and the smooth terms (for GAM) are null. In the case of MARS, the removed variables
 268 are those yielding to the most significant decrease in the GCV score. For the aim of
 269 simplicity, the predictor variables selected with the backward stepwise regression
 270 approach applied to the quantile associated to the smallest return period are considered as
 271 predictor variables to estimate the other quantiles. Ouarda et al. (2018) suggested that the
 272 quantile with the smallest return period can be considered as the most reliable quantile.

273 **3.3 Validation**

274 The performances of each considered RFA combination are assessed using a jackknife
 275 procedure. This method consists in considering, in turn, each gauged site as the target site
 276 and performs RE. This process is repeated for each gauged site. Then, the regional
 277 estimate is compared to its corresponding observed value. Based on the jackknife
 278 procedure, a number of standard performance criteria can be used to evaluate the
 279 prediction power of each regional model:

Nash- Sutcliffe Efficiency index:

$$\text{NASH} = 1 - \frac{\sum_{i=1}^N (y_i - \hat{y}_i)^2}{\sum_{i=1}^N (y_i - \bar{y})^2} \quad (9)$$

Root-mean-square error :

$$\text{RMSE} = \sqrt{\frac{1}{N} \sum_{i=1}^N (y_i - \hat{y}_i)^2} \quad (10)$$

Relative root-mean-square error :

$$\text{RRMSE} = 100 \sqrt{\frac{1}{N} \sum_{i=1}^N \left[\frac{(y_i - \hat{y}_i)}{y_i} \right]^2} \quad (11)$$

Mean bias :

$$\text{BIAS} = \frac{1}{N} \sum_{i=1}^N (y_i - \hat{y}_i) \quad (12)$$

Relative mean bias :

$$\text{RBIAS} = 100 \frac{1}{N} \sum_{i=1}^N \frac{(y_i - \hat{y}_i)}{y_i} \quad (13)$$

280 where y_i and \hat{y}_i are, respectively, the local and regional quantile estimates at site i , \bar{y} is
281 the mean of the local quantile estimates, and N is the number of stations.

282 Based on the computed performance criteria, the best models can be identified and then
283 used to make predictions in the ungauged sites of the study case.

284 **4. Case study and datasets**

285 Considering a number of physio-meteorological variables (Table 2), the considered
286 regional approaches are applied to a group of hydrometric stations located in the southern
287 part of Quebec (Canada) within a radius of 250 kilometres around the city of Montreal
288 (Figure 1). The objective is to estimate the specific flood quantiles QS_T (with $T = 10, 50$
289 and 100 years) for the spring season (January-June) at ungauged sites. The considered
290 region is characterized by its low number of hydrometric stations.

291 In this study, we focus on the spring season because maximum annual floods in the study
292 area often occur on this season. Figure 2 illustrates the variation of the annual mean of
293 the day's indices associated to the maximum annual flow as a function of the sites. It can
294 be seen that annual floods occur generally during the spring season and especially
295 between the April and May months, hence the choice to focus on this season.

296 The hydrological variables are calculated from daily flows acquired by the Quebec Water
297 Expertise Center (CEHQ) available at
298 (https://www.cehq.gouv.qc.ca/hydrometrie/historique_donnees/default.asp). Considering
299 a number of selection criteria such as the minimum size of the sample series at the station
300 (15 years), their monitoring levels (proximity to a natural regime with a maximum of an
301 influence on a daily basis) and their geographical proximity to the target stations, 63
302 hydrometric stations are retained for the estimation of the local quantiles.

303 A local frequency analysis (FA) is carried out in each gauged site. This involves the
304 verification of the basic assumptions (independence and stationarity) and the
305 identification of the adequate distributions. The distributions that are found to best fit the
306 observed data are essentially the two-parameter distribution functions such as gamma,
307 Weibull and the log normal. Finally, 57 stations are retained for the analysis of the QS_T
308 for the spring season.

309 The physio-meteorological variables used in this study come from widely validated and
310 used dataset covering the South of the province of Quebec (e.g. Shu and Ouarda 2007;
311 Durocher, Chebana, and Ouarda 2015; Wazneh, Chebana, and Ouarda 2016; Ouali,
312 Chebana, and Ouarda 2016) and are given in Table 2. The characteristics of catchments
313 corresponding to each gauged station are computed using the ArcHydro and HecGeoHms
314 tools implemented in the ArcGIS environment. These tools comprise functionalities for
315 catchment delineation and drainage network extraction from Digital Elevation Models
316 (DEMs). The DEMs used here are obtained from the Natural Resources Canada database
317 ([https://www.nrcan.gc.ca/earth-sciences/geography/topographic-information/download-](https://www.nrcan.gc.ca/earth-sciences/geography/topographic-information/download-directory-documentation/17215)
318 [directory-documentation/17215](https://www.nrcan.gc.ca/earth-sciences/geography/topographic-information/download-directory-documentation/17215)) distributed with a spatial resolution of ~ 20 m grid cells.

319 The DEMs of the United States Geological Survey (USGS)
320 (<https://earthexplorer.usgs.gov/>) are used for the cross-border catchments. These data
321 have a spatial resolution of ~ 30 m grid cells.

322 The catchment limit features are used to calculate the spatial average of the physio-
323 meteorological variables. The variables characterizing the drainage network systems are
324 extracted using the D8 method (O'Callaghan and Mark 1984; Jenson and Domingue
325 1988). The variables related to the land cover, are calculated based on the digital maps of
326 Quebec also available in the Natural Resources Canada database. The meteorological
327 variables are computed using spatial interpolation of the meteorological data of the
328 Ministry of the Environment and the Fight against Climate Change (MELCC). The
329 meteorological stations which retained in this study had at least 15 years of data. The
330 universal kriging method (Isaaks and Srivastava 1989) is used in this work for the spatial
331 interpolation of the meteorological data. This technique gave the most accurate
332 predictions based on a cross validation method. Descriptive characteristics of the
333 considered hydrological and physio-meteorological variables are summarized in Table 3.
334 It should be noted that, in this work a specific RT (RT standardized by basin area) is used
335 to eliminate the scale effect as RT is a variable that is highly correlated with the basin
336 area.

337 **5. Results and discussion**

338 *5.1 Delineation with CCA and ROI*

339 The CCA and the ROI approaches are applied in this study in the DHR using a set of
340 explanatory variables selected by a stepwise procedure. Given the complexity of GAM

341 and the small number of stations, 6 variables are used to model the spring flood quantiles
342 and 3 knots are considered in this model in the smooth functions. Based on these
343 parameters, the optimal threshold distance for the CCA and the ROI neighborhoods is
344 fixed at 5×10^{-6} and 6, respectively.

345 CCA requires the normality of the hydrological and physio-meteorological variables. To
346 achieve normality, some variables need to be transformed. The normality of each variable
347 is visually evaluated with a normal probability plot. This technique plots empirical
348 quantiles versus theoretical Gaussian quantiles and the plot should be approximately
349 linear in the case of actual normality. Visual inspection of transformed variables indicates
350 that the logarithmic transformation is applied to the flood quantiles, RT and MBS and a
351 square root transformation is used for PLAKE.

352 *5.2 Selection of optimal explanatory variables*

353 To avoid overfitting and optimise the predictive power of the methods, we perform
354 variable selection through backward stepwise techniques. The optimal variables selected
355 for the LLRM are RT, PLAKE, LONGC, ρ_{WMRB} , MBS, LATC and FS. For GAM, the
356 most relevant explanatory variables were found to be somewhat different than those
357 obtained for the LLRM because in this case selected predictors present non-linear links
358 with the response variables. These variables are namely, MCL, MBS, PFOR, PLAKE,
359 MASP and ρ_{WMRB} . Finally, the significant explanatory variables selected for MARS are
360 AREA, PLAKE, MALPS, RT, PFOR, MASP, ρ_{WMRB} and WMRB. The definition of
361 these variables is given in Table 2.

362 The selected variables mainly include: i) variables dealing with drainage network
363 characteristics such as RT, ρ_{WMRB} and WMRB. These variables have a high relationship
364 with the underlying lithology, the infiltration ability and the topographic characteristics of
365 the terrain which allow integrating more information about the underlying
366 hydrogeological flows (Msilini, Ouarda, and Masselot 2021); ii) Precipitations (MALPS
367 and MASP) and variables related to the local climate conditions such as LONGC and
368 LATC; and iii) variables characterising the land cover such as PLAKE acting like a
369 sponge absorbing the excess of water during the extreme events and PFOR variable
370 controlling the soil erosion phenomenon and the infiltration ability of the basins.

371 *5.3 Comparison of regional models*

372 Table 4 shows the jackknife validation results for each regional model. Accordingly, the
373 lowest RRMSE values are associated with the CCA/MARS approach, followed by
374 MARS and GAM applied with all datasets. With ALL, MARS has a comparable or even
375 superior performance than GAM. One can also see that, applying the LLRM model
376 within the neighborhoods gives considerably improved results. However, it did not
377 improve significantly the predictive ability of non-linear RE models, especially GAM.
378 This may be attributed to the fact that the amount of data used in this study is not
379 sufficiently large. On the other hand, the use of the neighborhood approaches often leads
380 to significant improvement in the RE in comparison with ALL. In this study, when non-
381 linear RE models are used, especially GAM, the difference between ALL and
382 neighborhood approaches is negligible. This result indicates that the use of non-linear RE
383 models may make the analyses more satisfactory and robust by compensating the benefits
384 of using the neighborhoods approaches which is not the case for the LLRM. Therefore,

385 non-linear RE models, especially GAM, seem especially useful for smaller datasets. The
386 use of these models may reduce the importance of using the neighborhood approaches.
387 In this work, the considered limited amount of data may also be the cause of the high
388 variance observed for the different models. It can also be seen that the NASH obtained
389 with the different approaches is not sufficiently high, especially for QS_{50} and QS_{100} . This
390 result may also be explained by the small size of the used data as the NASH is a criterion
391 that is highly sensitive to the sample size (McCuen, Knight, and Cutter 2006).

392 Figure 3 shows the variability of the relative error as a function of the sites associated to
393 the best models ALL/GAM, ALL/MARS and CCA/MARS for QS_{50} (QS_{10} and QS_{100} are
394 not presented here because of the similarity of the results). Overall, CCA/MARS
395 performs slightly better than the other approaches, especially for two specific sites that
396 have exceptionally large relative errors. The first site (050701) was also previously
397 identified by Ouali, Chebana, and Ouarda (2017) as a problematic station with atypically
398 large relative errors; the second site (030919) is a cross-border catchment. In this study,
399 the physiographical variables of the cross-border catchments are extracted based on data
400 come from the USGS database, which have a different resolution than the DEMs
401 obtained from the Natural Resources Canada database. This difference in measurement
402 might therefore explain this observation different behaviour.

403 The best models identified in this study are used to do predictions in the 11 ungauged
404 sites of the study case (see Figure 1). The estimations of the quantiles obtained by
405 CCA/MARS are found to be higher compared to those obtained by ALL/GAM and
406 ALL/MARS. This may be explained by the fact that the CCA/MARS approach presented
407 a positive RBIAS, and then it overestimates the target quantiles.

408 **6. Conclusions**

409 In this study, the performances of a number of commonly used regional approaches are
410 compared for the estimation of spring flood quantiles at 11 ungauged sites of interest
411 located in the Montreal region (Canada). The objective is to test the robustness of the
412 various methods by testing them on a real world case study with less than ideal
413 conditions: limited number of stations and moderate data quality. Different RE models
414 (LLRM, GAM and MARS) are considered with and without delineation methods (CCA
415 and ROI). These models are calibrated and validated on a group of catchments from the
416 study area. The best models are selected and used to estimate the flood quantiles at the
417 target ungauged sites.

418 Results indicate that it is possible and important to use the proposed non-linear regional
419 models in practice (GAM and MARS) because performances are improved when these
420 models are used instead of LLRM. The CCA/MARS combination was found to be the
421 best combination of DHR and RE with respect of the RMSE and RRMSE for this case
422 study. The neighborhood approaches considered in conjunction with GAM do not lead to
423 improved performances. This may be explained by the fact that the calibration of GAM
424 requires a large dataset which is not the case for the present study area. The different
425 models are also found to have a high variance compared to the bias, which may also be
426 attributed to the size and quality of the used dataset.

427 In future efforts, it may be of interest to enlarge the database by considering other stations
428 with short time series. Procedures for the combination of local and regional information
429 can then be used and their performance assessed (see for instance, Seidou et al. (2006)).

430 These procedures have been proposed in the literature but are almost never used in
431 practice. Their application to a real-world case study may help demonstrate their potential
432 and increase their use in practical hydrological estimation studies. One important aspect
433 that can also be considered in future work is the integration of climate change influence
434 in the modeling of the hydrological response. Indeed, it would be of interest to test the
435 proposed statistical model using flood quantiles estimated under a changing climate. In
436 future efforts it may also be useful to assess and compare the predictions that were
437 obtained with the considered models with those obtained with deterministic models such
438 as HYDROTEL or CEQUEAU. In this work, we assessed and applied the different RE
439 models (LLRM, GAM and MARS) in combination with linear neighborhood models
440 (CCA and ROI). In further work, it should be of interest to evaluate and apply these
441 models in conjunction with non-linear neighborhood approaches such as the non-linear
442 canonical correlation analysis model (Ouali, Chebana, and Ouarda 2016) and the
443 nonlinear neighborhood approach based on statistical depth functions (Wazneh, Chebana,
444 and Ouarda 2016).

445

446 **Acknowledgments**

447 Financial support for this work was graciously provided by the Natural Sciences and
448 Engineering Research Council of Canada (NSERC), the Canada Research Chairs
449 program (CRC), the Regional County Municipality of Vaudreuil-Soulanges (MRC-
450 VS), the Communauté Métropolitaine de Montréal (CMM) and the Tunisian University
451 Mission in North America (MUTAN). The authors are grateful to Natural Resources
452 Canada and the USGS services for the DEM and digital data used, and to the info-climat

453 service of the Ministry of the Environment and the Fight against Climate Change of
454 Quebec (MELCC) for the hydrological and meteorological data used. The authors would
455 also like to thank Michel Leclerc, Simon Bellemare (MRC-VS) and Pierre Dupuis
456 (CMM) for their comments and contributions throughout the study.

457

458

459

460

461

462

463

464

465

466

467

468

469

470

471

472

473

474

475 **References**

- 476 Bayentin, Lampouguin, Salaheddine El Adlouni, Taha BMJ Ouarda, Pierre Gosselin, Bernard
477 Doyon, and Fateh Chebana. 2010. "Spatial variability of climate effects on ischemic heart
478 disease hospitalization rates for the period 1989-2006 in Quebec, Canada." *International*
479 *journal of health geographics* 9 (1):5. doi: <https://doi.org/10.1186/1476-072X-9-5>.
- 480 Burn, D. H. 1990. "Evaluation of regional flood frequency analysis with a region of influence
481 approach." *Water Resources Research* 26 (10):2257-65. doi:
482 <https://doi.org/10.1029/WR026i010p02257>.
- 483 Chebana, Fateh, Christian Charron, T. B.M.J Ouarda, and Barbara Martel. 2014. "Regional
484 frequency analysis at ungauged sites with the generalized additive model." *Journal of*
485 *Hydrometeorology* 15 (6):2418-28. doi: <https://doi.org/10.1175/JHM-D-14-0060.1>.
- 486 Chebana, Fateh, and Taha BMJ Ouarda. 2008. "Depth and homogeneity in regional flood
487 frequency analysis." *Water Resources Research* 44 (11). doi:
488 <https://doi.org/10.1029/2007WR006771>.
- 489 Dalrymple, T. 1960. *Flood-frequency analyses*. US Geological Survey Water Supply Paper
490 1543A: USGPO.
- 491 Durocher, Martin, Fateh Chebana, and Taha BMJ Ouarda. 2015. "A nonlinear approach to
492 regional flood frequency analysis using projection pursuit regression." *Journal of*
493 *Hydrometeorology* 16 (4):1561-74. doi: <https://doi.org/10.1175/JHM-D-14-0227.1>.
- 494 Friedman, Jerome H. 1991. "Multivariate adaptive regression splines." *The annals of statistics*:1-
495 67.
- 496 Gal, Yarin, and Zoubin Ghahramani. 2016. A theoretically grounded application of dropout in
497 recurrent neural networks. Paper presented at the Advances in neural information
498 processing systems.
- 499 GREHYS. 1996. "Presentation and review of some methods for regional flood frequency
500 analysis." *Journal of hydrology(Amsterdam)* 186 (1-4):63-84.
- 501 Han, Xudong, Taha BMJ Ouarda, Aatur Rahman, Khaled Haddad, Rajeshwar Mehrotra, and
502 Ashish Sharma. 2020. "A Network Approach for Delineating Homogeneous Regions in
503 Regional Flood Frequency Analysis." *Water Resources Research* 56
504 (3):e2019WR025910.
- 505 Hastie, and R. Tibshirani. 1987. "Generalized Additive Models: Some Applications." *Journal of*
506 *the American statistical Association* 82 (398):371-86. doi:
507 10.1080/01621459.1987.10478440.
- 508 Isaaks, EH, and RM Srivastava. 1989. "An Introduction to Applied Geostatistics, New York:
509 Oxford Univ." In.: Press.
- 510 Jenson, Susan K, and Julia O Domingue. 1988. "Extracting topographic structure from digital
511 elevation data for geographic information system analysis." *Photogrammetric*
512 *engineering and remote sensing* 54 (11):1593-600.
- 513 Khalil, B, TBMJ Ouarda, and A St-Hilaire. 2011. "Estimation of water quality characteristics at
514 ungauged sites using artificial neural networks and canonical correlation analysis." *Journal of Hydrology* 405 (3-4):277-87.
- 516 Lawrence, Steve, and C Lee Giles. 2000. Overfitting and neural networks: conjugate gradient and
517 backpropagation. Paper presented at the Proceedings of the IEEE-INNS-ENNS
518 International Joint Conference on Neural Networks. IJCNN 2000. Neural Computing:
519 New Challenges and Perspectives for the New Millennium.
- 520 Leitte, Arne Marian, Cristina Petrescu, Ulrich Franck, Matthias Richter, Oana Suciu, Romanita
521 Ionovici, Olf Herbarth, and Uwe Schlink. 2009. "Respiratory health, effects of ambient
522 air pollution and its modification by air humidity in Drobeta-Turnu Severin, Romania."

523 *Science of The Total Environment* 407 (13):4004-11. doi:
524 <https://doi.org/10.1016/j.scitotenv.2009.02.042>.

525 López-Moreno, Juan I, and David Nogués-Bravo. 2005. "A generalized additive model for the
526 spatial distribution of snowpack in the Spanish Pyrenees." *Hydrological Processes: An*
527 *International Journal* 19 (16):3167-76.

528 McCuen, Richard H, Zachary Knight, and A Gillian Cutter. 2006. "Evaluation of the Nash–
529 Sutcliffe efficiency index." *Journal of hydrologic engineering* 11 (6):597-602.

530 Milborrow, Stephen. 2018. "Derived from MDA: mars by Trevor Hastie and Rob Tibshirani. Uses
531 Alan Miller's Fortran utilities with Thomas Lumley's leaps wrapper. Earth: Multivariate
532 Adaptive Regression Splines . R package version 4.6.3."

533 Msilini, A, TBMJ Ouarda, and P Masselot. 2021. "Evaluation of additional physiographical
534 variables characterising drainage network systems in regional frequency analysis, a
535 Quebec watersheds case-study." *Stochastic environmental research and risk*
536 *assessment*:1-21.

537 Msilini, A., P. Masselot, and T.B.M.J. Ouarda. 2020. "Regional Frequency Analysis at Ungauged
538 Sites with Multivariate Adaptive Regression Splines." *Journal of Hydrometeorology*:1-
539 doi: 10.1175/jhm-d-19-0213.1.

540 O'Callaghan, John F, and David M Mark. 1984. "The extraction of drainage networks from digital
541 elevation data." *Computer vision, graphics, and image processing* 28 (3):323-44. doi:
542 [https://doi.org/10.1016/S0734-189X\(84\)80011-0](https://doi.org/10.1016/S0734-189X(84)80011-0).

543 Ouali, Dhouha, Fateh Chebana, and T.B.M.J Ouarda. 2016. "Non-linear canonical correlation
544 analysis in regional frequency analysis." *Stochastic environmental research and risk*
545 *assessment* 30 (2):449-62. doi: <https://doi.org/10.1007/s00477-015-1092-7>.

546 ———. 2017. "Fully nonlinear statistical and machine-learning approaches for hydrological
547 frequency estimation at ungauged sites." *Journal of Advances in Modeling Earth Systems*
548 9 (2):1292-306. doi: <https://doi.org/10.1002/2016MS000830>.

549 Ouarda, T.B.M.J, Claude Girard, George S Cavadias, and Bernard Bobée. 2001. "Regional flood
550 frequency estimation with canonical correlation analysis." *Journal of Hydrology* 254
551 (1):157-73. doi: [https://doi.org/10.1016/S0022-1694\(01\)00488-7](https://doi.org/10.1016/S0022-1694(01)00488-7).

552 Ouarda, T.B.M.J. 2016. "Regional flood frequency modeling." *chapter 77, in: V.P. Singh, (Ed).*
553 *Chow's Handbook of Applied Hydrology, 3rd Edition, Mc-Graw Hill, New York*:pp. 77.1-
554 .8, ISBN 978-0-07-183509-1.

555 Ouarda, T.B.M.J., Christian Charron, Yeshewatesfa Hundecha, André St-Hilaire, and Fateh
556 Chebana. 2018. "Introduction of the GAM model for regional low-flow frequency
557 analysis at ungauged basins and comparison with commonly used approaches."
558 *Environmental Modelling & Software* 109:256-71. doi:
559 <https://doi.org/10.1016/j.envsoft.2018.08.031>.

560 Ouarda, T.B.M.J., Christian Charron, Prashanth R Marpu, and Fateh Chebana. 2016. "The
561 generalized additive model for the assessment of the direct, diffuse, and global solar
562 irradiances using SEVIRI images, with application to the UAE." *IEEE Journal of*
563 *Selected Topics in Applied Earth Observations and Remote Sensing* 9 (4):1553-66. doi:
564 <https://doi.org/10.1109/jstars.2016.2522764>.

565 Ouarda, T.B.M.J., and C Shu. 2009. "Regional low-flow frequency analysis using single and
566 ensemble artificial neural networks." *Water Resources Research* 45 (11). doi:
567 <https://doi.org/10.1029/2008wr007196>.

568 Rahman, Aatur, Christian Charron, Taha BMJ Ouarda, and Fateh Chebana. 2018. "Development
569 of regional flood frequency analysis techniques using generalized additive models for
570 Australia." *Stochastic environmental research and risk assessment* 32 (1):123-39. doi:
571 <https://doi.org/10.1007/s00477-017-1384-1>.

572 Seidou, O, TBMJ Ouarda, M Barbet, P Bruneau, and B Bobee. 2006. "A parametric Bayesian
573 combination of local and regional information in flood frequency analysis." *Water*
574 *Resources Research* 42 (11). doi: <https://doi.org/10.1029/2005WR004397>.

575 Shu, Chang, and T.B.M.J. Ouarda. 2007. "Flood frequency analysis at ungauged sites using
576 artificial neural networks in canonical correlation analysis physiographic space." *Water*
577 *Resources Research* 43 (7). doi: doi:10.1029/2006WR005142.

578 Tasker, Gary D, Scott A Hodge, and C Shane Barks. 1996. "REGION OF INFLUENCE
579 REGRESSION FOR ESTIMATING THE 50-YEAR FLOOD AT UNGAGED SITES."
580 *JAWRA Journal of the American Water Resources Association* 32 (1):163-70. doi:
581 <https://doi.org/10.1111/j.1752-1688.1996.tb03444.x>.

582 Wazneh, Hussein, Fateh Chebana, and Taha BMJ Ouarda. 2016. "Identification of hydrological
583 neighborhoods for regional flood frequency analysis using statistical depth function."
584 *Advances in water resources* 94:251-63. doi:
585 <https://doi.org/10.1016/j.advwatres.2016.05.013>.

586 Wen, Li, Kerry Lee Rogers, Neil Saintilan, and Joanne Ling. 2011. "The influences of climate and
587 hydrology on population dynamics of waterbirds in the lower Murrumbidgee River
588 floodplains in Southeast Australia: implications for environmental water management."
589 *Ecological Modelling* 222 (1):154-63. doi:
590 <https://doi.org/10.1016/j.ecolmodel.2010.09.016>.

591 Wood. 2006. *Generalized additive models: an introduction with R*: CRC press.
592 ———. 2017. *Generalized additive models: an introduction with R*: CRC press.

593 Xu, Jianhua, Weihong Li, Minhe Ji, Feng Lu, and Shan Dong. 2010. "A comprehensive approach
594 to characterization of the nonlinearity of runoff in the headwaters of the Tarim River,
595 western China." *Hydrological Processes: An International Journal* 24 (2):136-46. doi:
596 <https://doi.org/10.1002/hyp.7484>.

597

598

599

600

601

602

603

604

605

606

607

608

Table 1 Considered regional models.

Step Regional model	DHR	RE
ALL/LLRM	ALL (all stations)	LLRM
ALL/GAM	ALL (all stations)	GAM
ALL/MARS	ALL (all stations)	MARS
CCA/LLRM	CCA	LLRM
CCA/GAM	CCA	GAM
CCA/MARS	CCA	MARS
ROI/LLRM	ROI	LLRM
ROI/GAM	ROI	GAM
ROI/MARS	ROI	MARS

610

611

Table 2 List of variables used in the present study.

Notation	Variable
QS _T	Spring specific flood quantiles associated to the return period T
AREA	Basin area
MCL	Main channel length
MCS	Main channel slope
MBS	Mean basin slope
PFOR	Percentage of the area occupied by forest
PLAKE	Percentage of the area occupied by lakes
MATP	Mean annual total precipitation
MALP	Mean annual liquid precipitation
MASP	Mean annual solid precipitation
MALPS	Mean annual liquid precipitation (summer–fall)
DDBZ	Mean annual degree days below 0 °C
LATC	Latitude of the centroid of the basin
LONGC	Longitude of the centroid of the basin
RT	Texture ratio
RC	Circularity ratio
MRL	Mean stream length ratio
MRB	Mean bifurcation ratio
WMRB	Weighted mean bifurcation ratio
ρ_{WMRB}	RHO WMRB coefficient
DD	Drainage density
FS	Stream frequency
IF	Infiltration number
RN	Ruggedness number
PN1	Percentage of first-order streams
PL1	Percentage of first-order stream lengths

612

613 **Table 3** Descriptive statistics of the hydrological and physio-meteorological variables.

Variable	Min	Mean	Max	Std. dev
AREA (km ²)	26.30	1045.85	5440	1196.13
MCL (km)	12.51	68.98	225.80	46.13
MCS (m/km)	0.77	4.23	21.06	3.94
MBS (degree)	0.26	3.00	9.72	2.05
PFOR (%)	5.15	67.45	96	24.99
PLAKE (%)	0.00	3.93	21.28	3.86
MATP (mm)	923	1066.47	1239	78.33
MALP (mm)	669	828.68	1097	73.23
MASP (cm)	166	252.61	343	41.46
MALPS (mm)	426	504.64	664	45.30
DDBZ (degree-day)	859	1167.19	1578	184.25
LATC (°N)	44.88	45.97	47.43	0.66
LONGC (°W)	70.65	72.88	75.12	1.14
RT (km ⁻¹)	2.42	16.40	45.25	9.84
RC	0.08	0.21	0.39	0.07
MRL	0.48	0.84	1.14	0.20
MRB	1.69	2.12	5.78	0.74
WMRB	1.85	2.06	2.86	0.18
ρ_{WMRB}	0.18	0.41	0.55	0.10
DD (km ⁻¹)	2.10	2.84	3.48	0.29
FS (km ⁻²)	7.04	9.10	11.42	1.21
IF (km ⁻³)	16.04	26.20	39.73	6.06
RN	0.05	1.56	3.70	0.85
PN1 (%)	50.16	50.39	51.20	0.22
PL1 (%)	38.78	51.59	60.43	4.47
QS ₁₀ (m ³ /s km ⁻²)	0.080	0.272	0.482	0.093
QS ₅₀ (m ³ /s km ⁻²)	0.108	0.346	0.679	0.135
QS ₁₀₀ (m ³ /s km ⁻²)	0.119	0.377	0.772	0.156

614

615

616

617

618

619

620

621

622

Table 4 Jackknife validation results (Best results are in bold character).

Quantile	LLRM			GAM			MARS		
	ALL	CCA	ROI	ALL	CCA	ROI	ALL	CCA	ROI
QS10	0.426	0.604	0.522	0.705	0.681	0.706	0.731	0.743	0.652
QS50	0.409	0.593	0.464	0.589	0.534	0.579	0.551	0.586	0.559
NASH QS100	0.383	0.575	0.419	0.521	0.468	0.510	0.426	0.558	0.486
QS10	0.070	0.058	0.064	0.050	0.052	0.050	0.048	0.046	0.054
QS50	0.103	0.085	0.099	0.085	0.091	0.086	0.089	0.085	0.088
RMSE [(m ³ /s)km ⁻²] QS100	0.122	0.101	0.119	0.107	0.113	0.108	0.117	0.102	0.111
QS10	29.020	25.610	26.712	21.796	21.290	21.353	19.023	17.189	22.607
QS50	29.933	27.785	29.078	28.476	28.637	28.196	26.857	21.385	26.532
RRMSE (%) QS100	31.456	29.508	30.933	31.863	32.017	31.602	32.514	23.723	29.529
QS10	0.003	0.009	0.005	0.004	0.007	0.001	0.007	0.013	-0.004
QS50	0.004	0.013	0.005	0.008	0.012	0.005	0.013	0.015	0.001
BIAS [(m ³ /s)km ⁻²] QS100	0.005	0.015	0.005	0.011	0.016	0.007	0.005	0.021	0.006
QS10	-3.819	-1.792	-2.535	-1.488	-0.815	-2.843	1.199	2.577	-4.377
QS50	-4.049	-2.218	-3.677	-2.331	-1.967	-4.005	-0.496	1.546	-4.628
RBIAS (%) QS100	-4.390	-2.584	-4.350	-2.946	-2.552	-4.834	-4.498	1.541	-3.865

623

624

625

626

627

628

629

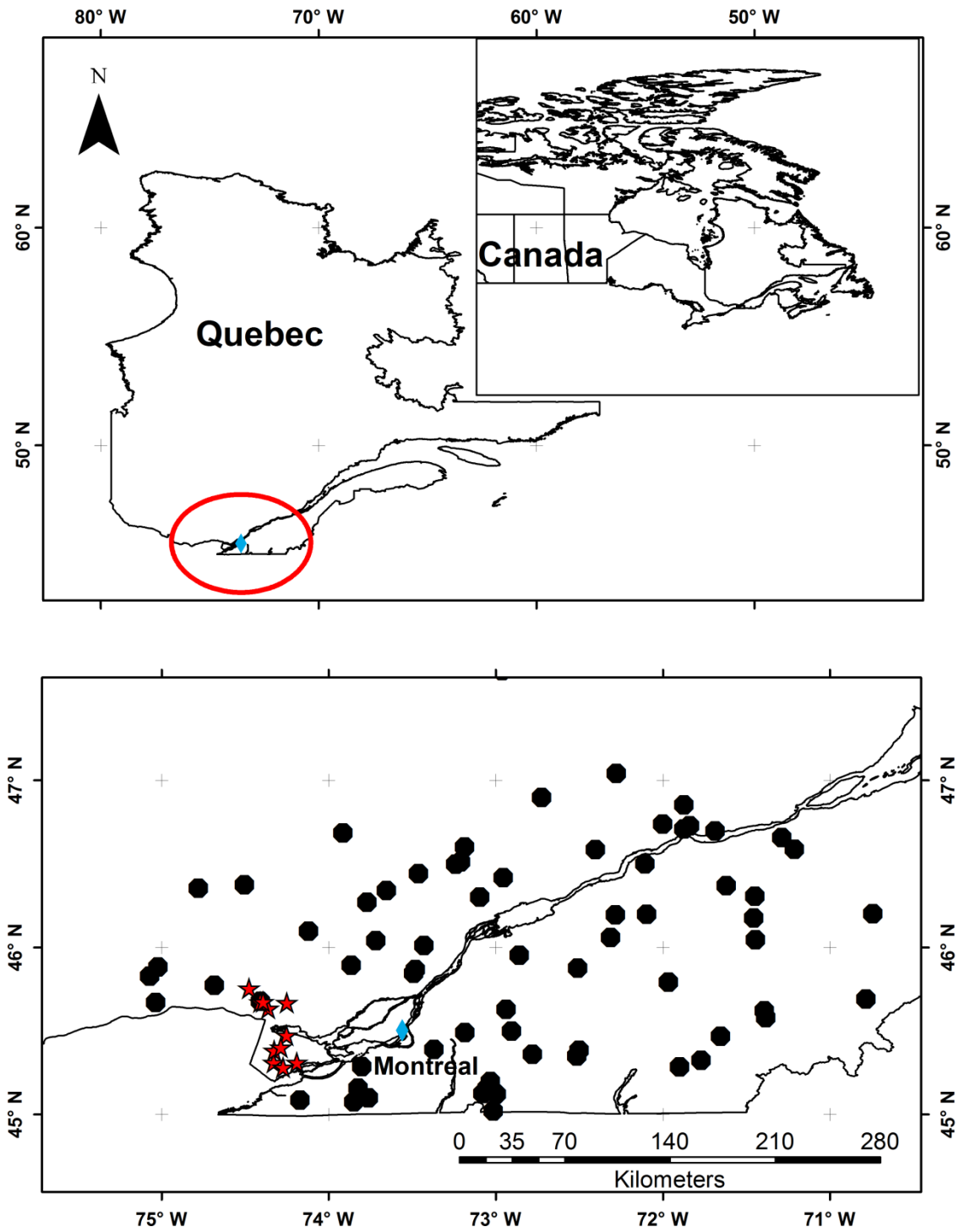
630

631

632

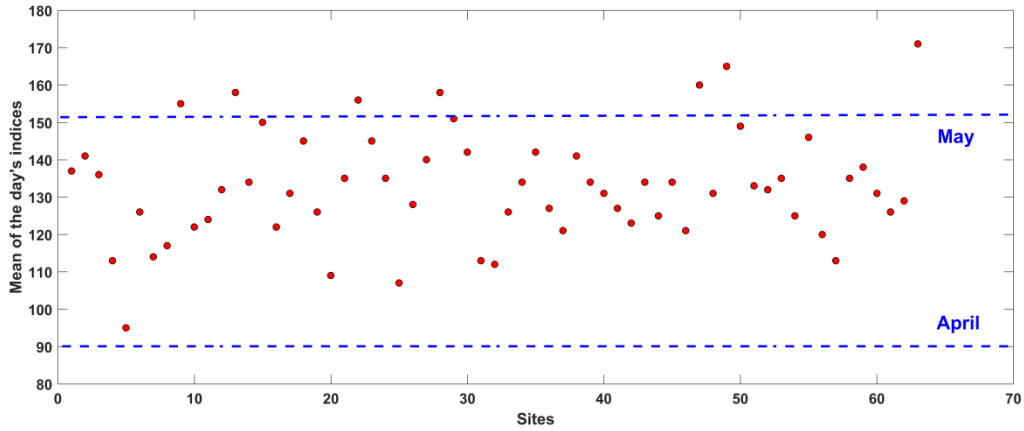
633

634



635
 636
 637
 638
 639
 640

Figure 1 Location of the hydrometric stations across the study area (black circles), the red stars present the ungauged sites. The blue diamond refers to the location of the study area (Montreal region).

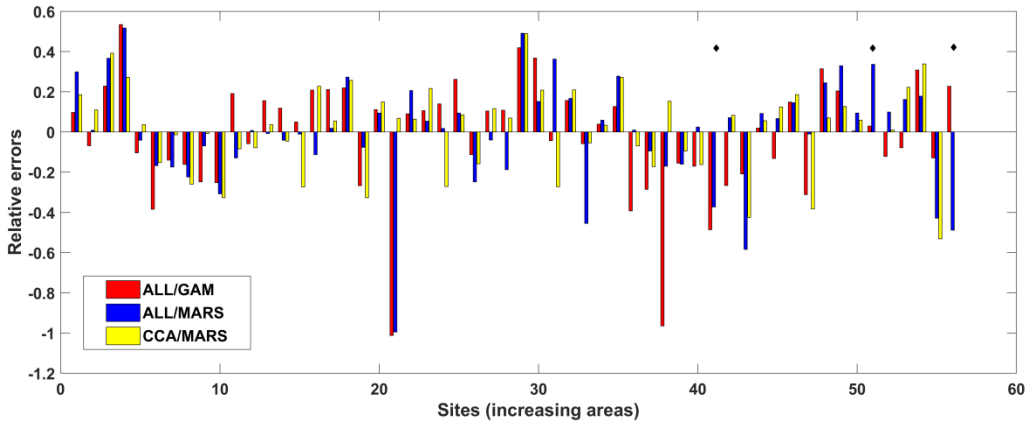


641

642 **Figure 2** Annual mean of the day's indices (MDI) associated to the maximum annual
 643 flow as a function of sites. The dotted blue lines represent the limit of the April-May
 644 months. The red circles are the MDI values (annual floods) which are mostly observed in
 645 the April-May months.

646

647



648

649 **Figure 3** Relative errors associated to the at site quantile QS50 calculated using
 650 ALL/GAM; ALL/MARS and CCA/MARS. Diamond refers to sites with (or not) a small
 651 neighborhood. Sites are ordered according to their areas.

652

653

654

655